

## Map Building for Indoor Tracked Autonomous Mobile Robot with Laser Rangefinder and Electronic Compass

Zhu Jianguo<sup>1+</sup>, Gao Junyao<sup>1</sup>, Li Kejie<sup>1</sup>, Ren Peijie<sup>1</sup> and Yin Qiang<sup>2</sup>

<sup>1</sup>School of Mechatronic Engineering, Beijing Institute of Technology, Beijing, China

<sup>2</sup>College of Mechanical Automation, Wuhan University of Science and Technology, Wuhan, China

**Abstract.** this paper describes a method of grid map building for indoor tracked autonomous mobile robot (AMR) equipped with 2D laser rangefinder and electronic compass. Grid map for the indoor environment is built by the mobile robot. Grid map is widely used in mobile robot navigation tasks such as robot localization and path planning. Map building technology is indispensable for mobile robot to execute exploration task in unknown environment.

Firstly, different type of maps as presentation of environment model are discussed and compared; the tracked AMR's hardware architecture is introduced. Secondly, robot's kinematics model is established; the main sensors' (laser rangefinder, electronic compass, odometer and infrared sensors) models are analyzed; the methods of data acquisition are presented. Thirdly, the process of building grid map is described in detail, in which multi-sensors data fusion is implemented. Finally, maps building experiments is done in the corridor and the office of the laboratory. Results demonstrate the map building method is effective and suitable for the mobile robot to perform complex tasks in partially known or completely unknown environments.

**Keywords-**map building; autonomous mobile robot(AMR); laser rangefinder; electronic compass; data fusion

### 1. Introduction

Autonomous exploration skill is an extremely important capability for AMR. For example, assume that several hostages are trapped in a room of a building by armed terrorists or criminals. Under such dangerous circumstance, an AMR capable of environment-auto-exploring been sent to the building first by the police will make things much easier. If possible, an armed AMR can rescue hostages by shooting terrorists. So capability of building maps of an unknown environment without human intervention is desired for AMR to complete autonomous exploration task that includes self-localization, path planning, obstacle avoidance and target reaching.

Generally speaking, the map models built by mobile robots can be classified into the following four paradigms (see Fig. 1). The first one is place recognition whose map consists of a list of places that can be recognized by robot. The second model is topological map in which the environment is represented as a graph of connected places. The third one is metric map in which the environment is represented as a set of objects with coordinates in 2D space. In particular, grid map and feature-based map are the two most common metric map models and in this paper grid map building with a new method is described in detail. The last one is metric topological map in which the environment is represented by a set of distinctive landmarks and places.

---

<sup>+</sup> E-mail address: gaojunyao@bit.edu.cn

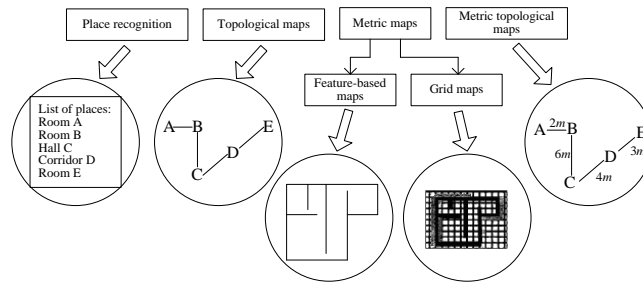


Figure 1. Different type of map models



Figure 2. The physical structure of the tracked AMR

The tracked mobile robot for mapping building is a differential drive type robot with six tracks as shown in Fig. 2. Two main tracks are driver tracks to drive left and right wheels independently. Four tracked arms make robot be able to climb the stairs. An accurate 2D laser rangefinder URG-04LX is mounted in the front of robot as the main environment modeling sensor. Inside the robot, a PC104 is selected as the robot's main controller that executes complex tasks. In the back of robot, there is an electronic compass XW-EC1700 that provides 3D orientation of the robot. If wish to obtain more information of robot, a miniature, gyro-enhanced Attitude and Heading Reference System (AHRS) named MTi can take place of XW-EC1700. Its internal low-power signal processor provides drift-free 3D orientation as well as calibrated 3D acceleration, 3D rate of turn (rate gyro) and 3D earth-magnetic field data. Infrared range sensors ring mounted around robot body are also used for obstacles avoidance. Three cameras are installed at different places enable the robot to have a full view of the ambient environment. A GPS is optional for the robot's general positioning if the outdoor environment applications are carried out.

The robot system adopts hierarchical control structure as shown in Fig. 3. The PC104 is used as the central controller by which all sensors' information are gathered together and all the complex tasks, such as self-localization, map building, path planning, obstacles avoidance, strategies decision and fault diagnose, are all accomplished. Four Programmable controllers (PLC) are at bottom of the control structure and have different tasks. PLC1 mainly takes responsible of retransmitting command frames and information frames between the top layer's PC104 and the bottom layer's PLCs through RS485 bus. In addition, it selects which camera connects to the video transmitter according to the received command. PLC2 controls two main motors to driver main tracks and plays roll in avoiding collision through the infrared range sensors. PLC3 manages front and rear arms' motion which enable robot be able to climb up and down the stairs. PLC4 receives GPS information such as longitude and latitude for robot's coarse positioning in Google Map (It is optional for outdoor application).

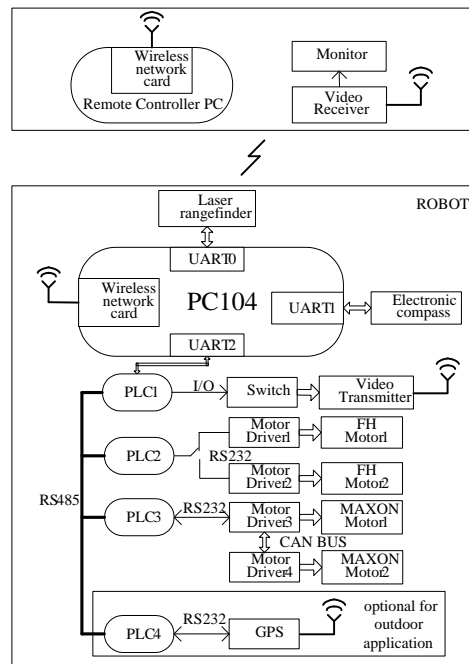


Figure 3. The overall structure of the tracked AMR

## 2. Kinematics Modeling of Robot and Sensors Equipment Description

As the task of map building can't be done without robot's self localization and internal and external sensors' information. In this section, the kinematics model of tracked mobile robot is established and the main sensors, such as motor encoders, laser rangefinder, electronic compass and infrared range sensors are described.

### 2.1. Kinematic Model of Tracked Mobile Robot

This AMR is a differential driven type robot with two independent main driven tracks mounted on the left and right hand sides of the robot. Compared with wheeled mobile robots of differential driven type, tracked mobile robot is subject to transverse friction while it is turning. In addition, its trajectory is decided not only by control input, but also by the ground condition and the robot's current steering status.

The following assumptions are imposed in the robot and its motion:

- Robot moves in the 2D planar space.
- The length of the main tracks touched with ground is the same. Their width is also equal to each other.
- The line connects both main tracks' center is perpendicular to the direction of robot's movement.
- Robot has rigid shell and two main tracks touch with the ground closely.

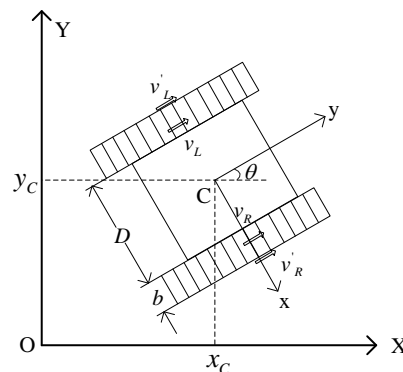


Figure 4. The schematic diagram of robot motion

Based on assumptions listed above, the robot' pose can be defined by vector  $P = [x_c, y_c, \theta_c]^T$ , where  $(x_c, y_c)$  is the Cartesian coordinate of robot's mass center and  $\theta_c$  is the heading angle (see Fig. 4).  $D$

represents the width of robot body and  $b$  is the width of single track. Assume that the theoretical speeds of left and right wheel are  $v_L$  and  $v_R$  respectively. Then the kinematics model of the tracked robot can be given by

$$\begin{cases} \dot{x}_C = \frac{1}{2} [v_L(1-k_L) + v_R(1-k_R)] \cos \theta_C \\ \dot{y}_C = \frac{1}{2} [v_L(1-k_L) + v_R(1-k_R)] \sin \theta_C \\ \dot{\theta}_C = \frac{-v_L(1-k_L) + v_R(1-k_R)}{D+2b} \end{cases} \quad (1)$$

Where  $k_L$  and  $k_R$  are slip rates of left and right tracks and can be calculated by the equations bellow:

$$k_L = \frac{v_L - v'_L}{v_L}, k_R = \frac{v_R - v'_R}{v_R}. \quad (2)$$

$v'_L$  and  $v'_R$  are absolute speeds of left and right tracks. The theoretical speed is equal to absolute speed when tracks have no slippage in which case  $v_L = v'_L, v_R = v'_R$ . So when tracks' slipping is unconcerned, the kinematics model of robot can be simplified as follows:

$$\dot{P} = \begin{bmatrix} \dot{x}_C \\ \dot{y}_C \\ \dot{\theta}_C \end{bmatrix} = \begin{bmatrix} \frac{1}{2} \cos \theta_C & \frac{1}{2} \cos \theta_C \\ \frac{1}{2} \sin \theta_C & \frac{1}{2} \sin \theta_C \\ -\frac{1}{D+2b} & \frac{1}{D+2b} \end{bmatrix} \begin{bmatrix} v_L \\ v_R \end{bmatrix}. \quad (3)$$

## 2.2. Analysis of Odometer Model

The working principal of odometer is to calculate the relative changes of robot's pose according to the two encoders mounted on the motors' shafts. In other words, the distances of tracks moved can be obtained from rounds of motors rotated by equations bellow:

$$\begin{cases} \Delta S_L = (1-k_L) \times 2 \times (N/p) \times \pi r \\ \Delta S_R = (1-k_R) \times 2 \times (N/p) \times \pi r \end{cases} \quad (4)$$

Where  $\Delta S_L$  and  $\Delta S_R$  are the distances of the left and right track moved respectively. Besides,  $r$  represents the radius of the wheels wrapped with rubber tracks.  $N$  is the pulse counts outputted by encoder in a time period  $\Delta t$ .  $p$  denotes the resolution of encoders.  $k_L$  and  $k_R$  are slip rates of left and right tracks mentioned above.

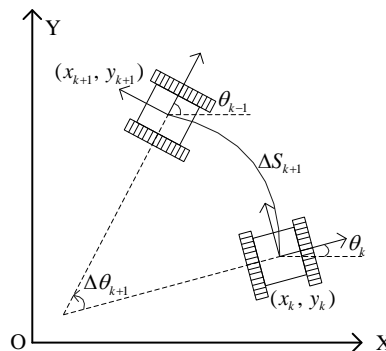


Figure 5. The arc model diagram of odometer

As shown in Fig. 5, assume that the mobile robot moves from an old pose  $X_k = [x_k, y_k, \theta_k]^T$  to a new one  $X_{k+1} = [x_{k+1}, y_{k+1}, \theta_{k+1}]^T$ , the distance of robot moved is  $\Delta S = (\Delta S_R + \Delta S_L) / 2$  and the angle of robot turned is  $\Delta \theta = (\Delta S_R - \Delta S_L) / (D+2b)$ . Then the arc model equation of odometer can be written as

$$X_{k+1} = f(X_k, u_{k+1}) = \begin{pmatrix} x_k + \frac{\Delta S_{k+1}}{\Delta \theta_{k+1}} (\sin(\theta_k + \Delta \theta_{k+1}) - \sin \theta_k) \\ y_k - \frac{\Delta S_{k+1}}{\Delta \theta_{k+1}} (\cos(\theta_k + \Delta \theta_{k+1}) - \cos \theta_k) \\ \theta_k + \Delta \theta_{k+1} \end{pmatrix}. \quad (5)$$

### 2.3. Analysis of Laser Rangefinder

The laser rangefinder selected is the Hokuyo URG-04LX scanning laser rangefinder. It is a small, affordable and accurate laser scanner that is perfect for robotic applications. It is able to report ranges from 20mm to 5600mm (1mm resolution) in a  $240^\circ$  arc ( $0.36^\circ$  angular resolution). It provides data for robot through RS232 or USB interface.

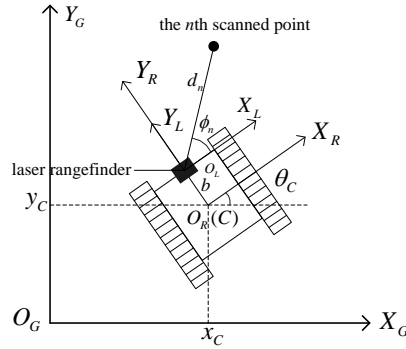


Figure 6. The schematic diagram of laser rangefinder ranging

The local pose of the  $n$ th laser rangefinder scanned point  $n=(1,2,\dots,N)$  is denoted by the polar coordinates  $s_n = (d_n, \phi_n)^T$ .  $N$  denotes the total number of laser rangefinder's scanned points. Its corresponding Cartesian coordinates in the laser rangefinder coordinate system is  $P^n_L = (x^n_L, y^n_L)^T = (d_n \cos \phi_n, d_n \sin \phi_n)^T$ . Its Cartesian coordinates  $P^n_R$  in the robot coordinate system can be calculated by left multiplying  $P^n_L$  by a transformation matrix as shown bellow.

$$P^n_R = \begin{bmatrix} x^n_R \\ y^n_R \end{bmatrix} = \begin{bmatrix} \cos \theta_L & -\sin \theta_L \\ \sin \theta_L & \cos \theta_L \end{bmatrix} \begin{bmatrix} x^n_L \\ y^n_L \end{bmatrix} + \begin{bmatrix} a \\ b \end{bmatrix}. \quad (6)$$

where  $[a, b, \theta_L]^T$  is the laser rangefinder's pose in robot coordinate system and is usually a constant vector after the laser rangefinder is mounted on the robot. For this robot,  $a=0, b=0.3m, \theta_L=0$ . In the same way, the Cartesian coordinates  $P^n_G$  of the  $n$ th scan point in global coordinate system can be given by

$$P^n_G = \begin{bmatrix} x^n_G \\ y^n_G \end{bmatrix} = \begin{bmatrix} \cos \theta_C & -\sin \theta_C \\ \sin \theta_C & \cos \theta_C \end{bmatrix} \begin{bmatrix} x^n_R \\ y^n_R \end{bmatrix} + \begin{bmatrix} x_C \\ y_C \end{bmatrix}. \quad (7)$$

where  $[x_C, y_C, \theta_C]^T$  is laser robot's current pose in global coordinate system. The schematic diagram of laser rangefinder ranging is shown in Fig. 6.

### 2.4. Analysis of Electronic Compass

Electric compass XW-EC1700 mainly outputs yaw angle, pitch angle and roll angle. Yaw angle is used to indicate robot's orientation together with wheel encoders by weighting as follows:

$$\Delta \theta = \lambda \Delta \theta_c + (1 - \lambda) \Delta \theta_e. \quad (8)$$

where  $\lambda$  and  $1-\lambda$  are weights of yaw angle variation measured by compass and encoders respectively. It is useful because the errors of orientation calculated by wheel encoders will grow with drift, bias or slippage and accumulate over time as integration errors. Furthermore, Robot can be prevented from overturning by real-time monitoring pitch angle and roll angle.

## 2.5. Analysis of Infrared Range Sensors

The infrared sensors are optoelectronic devices GP2Y0A02YK which outputs analog voltage. Its measurement range is from 20 to 150cm. PLC2 obtains the readings of all the infrared range sensors by adding an A/D converter. The output distance characteristics of GP2Y0A02YK are shown in Fig. 7.

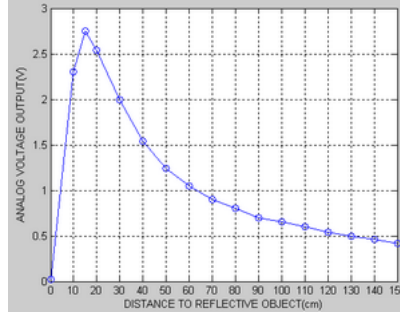


Figure 7. The output distance characteristics of the infrared sensors

## 3. Grid Map Building

The grid map is a probabilistic approach in which the environment is modeled by small grid cells. Each grid cell has an occupancy probability of an object. The grid map represents environments accurately by updating grid cells continuously and intuitively. Typical applications of the grid based map are global path-planning, navigation and target finding.

The process of grid map building can be divided into three steps. The first one is gathering robot's external and internal sensors' information; the second one is constructing the local grid map; the final step is updating the global grid map.

In the grid map solution, the grid map is divided into  $480 \times 360$  small grids, in which each grid represents  $0.2m \times 0.2m$  area in real world. Therefore, an area of  $96m \times 72m$  in real environment can be represented by the grid map and usually that is large enough for the robot's indoor applications. At initial, a uniform occupancy probability distribution  $p_{init} = 0.5$  is assigned to each grid cell, which means all area in map is unexplored and unknown.

### 3.1. Sensors' Data Acquisition and Processing

The laser rangefinder URG-04LX will reply with the latest measurement data of 228 scanning points according to the inquiring command sent by the PC104 each time. When an entire scanned data frame is received, invalidate data should be revised first because the effective measurement range of URG-04LX is between 20mm and 5600mm. Thus a distance threshold  $d_{th}$  is used to deal with the readings out of range:  $d_n = 5600mm$ , if  $d_n < d_{th}$ .

Furthermore, a corresponding flag bit that indicates no obstacle exists along the laser ray as far as  $d_n$  is set. And then the isolated noise should also be removed according to the rules shown bellow.

$$\begin{cases} d_n = \frac{d_{n-1} + d_{n+1}}{2}, & \text{if } d_{n-1} \neq 0, d_n = 0 \text{ and } d_{n+1} \neq 0 \\ d_n = 0, & \text{if } d_{n-1} = 0, d_n \neq 0 \text{ and } d_{n+1} = 0 \end{cases} \quad (9)$$

A comparison between laser rangefinder's scan images before and after isolated noise elimination is demonstrated in Fig. 8.

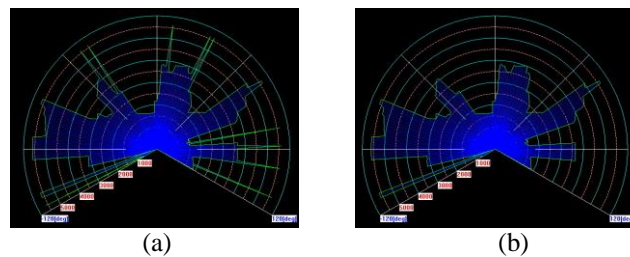


Figure 8. Laser rangefinder' scan images: (a) before noise elimination (b) after noise elimination

The encoders' readings for the robot's dead reckoning are obtained by inquiring PLC1 periodically. Other information such as main motors' speed, angles of arms, infrared sensors' readings and GPS data (optional for robot outdoor applications) are also received at the time. These data occupy different fields in the received information frame.

Besides, the yaw angle of robot is obtained directly from the electronic compass by PC104 through RS232 interface. Similarly, noise-filtering process is also indispensable to ensure orientation data correct and reliable.

### 3.2. Local Grid Map Building

Each time the sensor's information is updated, the robot pose  $P = [x_c, y_c, \theta_c]^T$  is calculated as described in detail in the second section immediately. In particular, yaw angle provided by the electronic compass plays an important roll in the final decision of  $\theta_c$  and this process can be called as sensors data fusion.

When a laser rangefinder scanned data frame is obtained, a local grid map is built according to robot latest pose. The process is described bellow and the flow chart of grid map building is summarized as shown in Fig. 10.

1) *Coordinates transformation of all scanned points:* For every scanned point of laser rangefinder, its polar coordinates  $s_n = (d_n, \phi_n)^T$  should be transformed to  $P^n_G = (x^n_G, y^n_G)^T$  in the global coordinates system firstly through equations listed in the second section. And then check whether the point belongs to the grid map or not. If not, some corresponding measures should be taken to make sure it won't bring any error in the following steps.

2) *Calculate the row and column number of the scanned points in the grid map:* Once the fact that the  $n$ th scanned point is in the range of the grid map is confirmed, calculate which grid it belongs to and derive the row and column number of the grid.

3) *Calculate the probability of corresponding grids that penetrated by the  $n$ th laser ray:* If the grid containing the scanned point is really occupied by the obstacle, its measurement probability  $p(z|x, m)$  is set to the default probability of obstacles area. And then the probability  $p(z|x, m)$  of those grids penetrated by the  $n$ th laser ray but without obstacles is equal to the default probability of blank area. The updated occupancy probability  $p(m|x, z)$  is determined by using the Bayes conditional probability theory as (10) according to the distance of the grid cell from the laser range finder, in which  $p(m)$  is occupancy probability of the grid in previous moment. The schematic diagram of calculate the grids' probability is shown in Fig. 9.

$$p(m|x, z) = p(z|x, m) \cdot p(m). \tag{10}$$

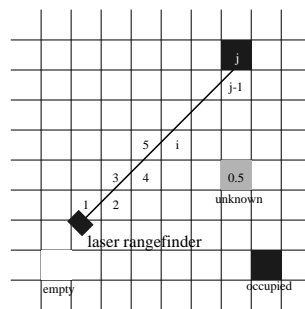


Figure 9. The schematic diagram of calculate grids' probability

### 3.3. Global Grid Map Updating

When a local grid map has been built, the work of updating the global grid map is done immediately. The updated occupancy probability is determined as shown in (10). The inverse measurement model of the static grid map is shown in table 1 in which empty means no obstacle, occupied represents there is obstacle and unknown implies the area has not been explored yet. In table 1,  $x^{t-1}$  is the previous moment status of a grid and  $z^t$  is its measurement status of current moment.

TABLE I. INVERSE MEASUREMENT MODEL OF GRID MAP

$x^{t-1}$		$z^t$
$p(z x, m)$		
empty	empty	low
unknown	empty	low
occupied	empty	low
empty	occupied	low
unknown	occupied	high
occupied	occupied	high

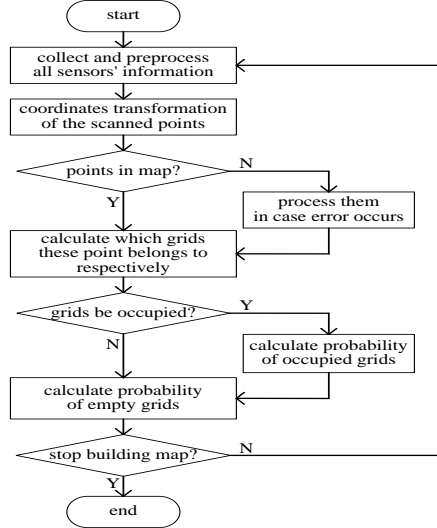
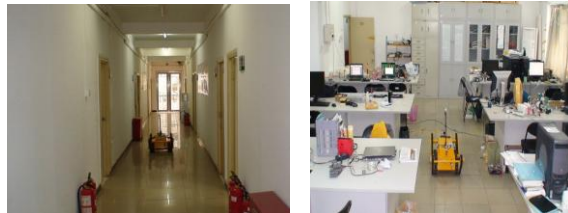


Figure 10. The flow chart of grid map building

#### 4. Experiments and Results

The grid map building experiments for the tracked mobile robot have been done in indoor environment by using method proposed above. The robot size is  $100cm \times 50cm \times 40cm$  and robot moved at a speed of  $0.3m/s$ . The sample frequencies of the laser rangefinder were  $5Hz$ . The electronic compass outputted 12 data frames per second.

Fig. 11 (a) is a picture of a corridor in which the mobile robot runs while building the grid map at the same time. And Fig. 11 (b) is the picture of an office. The corresponding map of the corridor built by robot is shown in Fig. 12. The process of the office map building is demonstrated in Fig. 13. It is worth mention that in some cases some blank grids are between the occupied grids in one laser ray. This is occurred when the occupied grid between laser rangefinder and the blank grid is only filled with thin obstacles such as legs of chairs. So other laser rays can penetrate the grid and detect obstacles behind it. The office's final grid map that had undergone some necessary revision is shown in Fig. 14.



(a) The corridor of lab      (b) the office

Figure 11. Experimental environments of grid map building



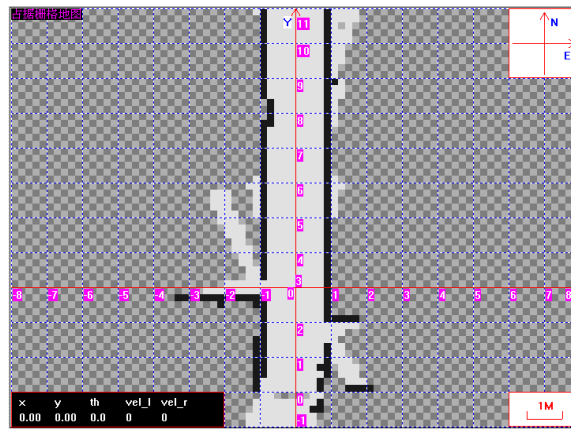


Figure 12. The grid map of the corridor built by AMR

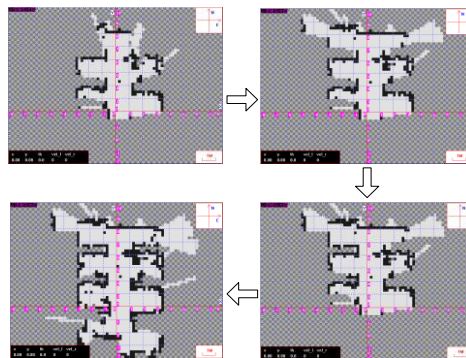


Figure 13. The process of the office grid map building

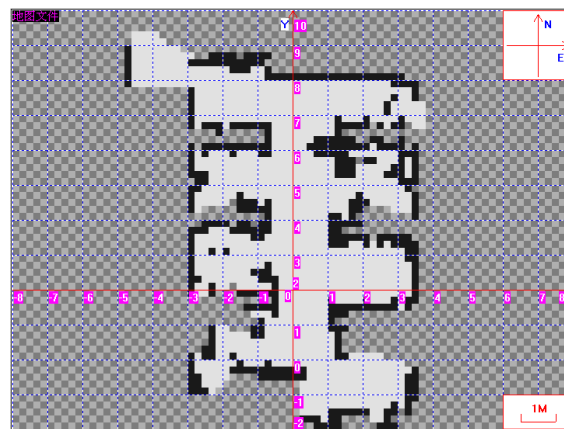


Figure 14. The final grid map of the office built by AMR

The experimental results show that the maps of the indoor environment built by the tracked AMR are accurate and useful for robot's future applications, such as environment exploration, navigation, obstacles avoidance tasks and so on.

## 5. Conclusion

This paper described the grid map building method with laser rangefinder and electronic compass installed on the tracked mobile robot. At the beginning, the kinematics model of track mobile robot and the model of several sensors used in the robot are analyzed. With the help of odometer and compass, the pose of the robot is determined through sensors' data fusion algorithm. And then the occupancy probability of every grid in the local grid map is calculated according to the laser rangefinder's scanned data. In the end of the sample period, the work of updating the global map to obtain the latest environment map is done. As the robot moving on, the indoor environment is modeled and its global grid map is constructed. In addition, the infrared

sensors ring mounted around the robot body is using to avoid collision when robot is moving to build map. Finally, the experiments were done and the results proved that the grid maps built by the AMR are accurate and suitable for robot's indoor environment applications.

## 6. Acknowledgment

I acknowledge School of Mechatronical Engineering of Beijing Institute of Technology. I would like to thank my tutors Prof. Li Kejie and Prof. Gao Junyao for their great help to my research.

## 7. References

- [1] HARA Yoshitaka, KAWATA Hirohiko, OHYA Akihisa, et al, "Map building for mobile robots using a SOKUIKI sensor-robust scan matching using laser relection intensity," proceedings of SICE-ICASE Internation Joint Conference 2006( SICE-ICCAS 2006). pp. 5951 - 5956, 18-21 Oct, 2006
- [2] Zezhong Xu, Jilin Liu, Zhiyu Xiang, et al, "Map building for indoor environment with laser range scanner," proceedings of the IEEE 5th International Conference on Intelligent Transportation Systems. pp. 136 - 140, 3-6 Sep, 2002
- [3] Elizabeth R. Stuck, Allan Manz, David A. Green, et al, "Map updating and path planning for real-time mobile robot navigation," proceedings of the 1994 IEEE/RSJ/GI International Conference on Intelligent Robots and Systems (IROS 1994). pp.753-760 vol.2, 12-16 Sep, 1994
- [4] Young-Hun Ki, Gu-Min Jeong, Chan-Woo, et al, "An indoor environment exploration technique for mobile robot using line segment histogram method," proceedings of the 2007 International Conference on Control, Automation and Systems (ICCAS 2007). pp.1136-1139, 17-20 Oct, 2007
- [5] Hongyu Cao, Hanxu Sun, Qingxuan Jia, et al, "Laser-scanner grid map building based on Dempster-Shafer evidence theory," proceedings of the 2009 IEEE International Conference on Mechatronics and Automation (ICMA 2009). pp.4930-4935, 9-12 Aug, 2009
- [6] Bingfeng Wang, Shigang cui, Li Zhao, et al, "Mobile robot map building based on grid arrangement," proceedings of the 2009 International Conference on Artificial Intelligence and Computational Intelligence (AICI 2009). pp.288-291, 7-8 Nov, 2009